Energy and Buildings 159 (2018) 529–541

Contents lists available at ScienceDirect

Energy and Buildings

journal homepage: www.elsevier.com/locate/enbuild

Analysis of operational performance of a mechanical ventilation cooling system with latent thermal energy storage

Thiago Santos[a,1], Chris Wines[a], Nick Hopper[b], Maria Kolokotroni[a,*]

[a] Institute of Energy Futures, Brunel University London, Kingston Lane, Uxbridge, UB8 3PH, UK
[b] Monodraught Ltd., Halifax House,Halifax Road, High Wycombe, UK

ARTICLE INFO

Article history:
Received 6 October 2017
Received in revised form
29 November 2017
Accepted 29 November 2017
Available online 1 December 2017

Keywords:
Active LTES
Operational performance
Cooling
Ventilation

ABSTRACT

Latent Thermal Energy Storage (LTES) is a promising solution to reduce cooling energy consumption in buildings. Laboratory and computational studies have demonstrated its capabilities while commercial passive and active systems are available. This paper presents data and analysis of the performance of an active LTES ventilation system in two case-studies, a seminar room and an open plan office in the UK. Analysis using environmental data from the system's control as well as additional space monitoring indicates that (a) internal temperature is maintained within adaptive thermal comfort limits, (b) acceptable Indoor Air Quality is also maintained (using metabolic CO_2 as indicator) and (c) energy costs are low compared to air-conditioned buildings. Thermal and CFD computational studies indicate that purging and charging duration and associated set-points for room temperature as well as air flow rate are the important parameters for optimised performance for a given LTES design. These parameters should be optimised according to the use of the space and prevailing external conditions to maintain internal thermal comfort within upper (usually in the afternoon) and lower (usually in the morning) limits.

1. Introduction

Energy storage is a very active area of research in recent years as it provides a sustainable solution to energy demand fluctuations and increases energy efficiency. Different energy storage methods such as mechanical energy storage (gravitational energy, flywheels); electrical storage (e.g. batteries); thermal storage (sensible, latent) and thermochemical heat storage [1] can be used. Thermal energy storage (TES) is particularly suited to buildings because a high percentage of their energy demand relates to heating and cooling needs. Sensible TES utilizes the heat capacity properties of materials while latent TES uses heat exchanges via the phase change of materials, usually between solid and liquid for building applications. Latent thermal energy storage (LTES) can provide more energy per volume than a sensible thermal storage system, making LTES a promising solution for buildings either integrated into building envelope (passive LTES) or in ventilation systems (active LTES) to reduce cooling demand [2] or reduce heating demand [3].

Active LTES integrated in mechanical ventilation systems has received attention during the last two decades. A room ventilation system incorporating heat pipes embedded in PCM thermal battery was tested experimentally for applications in the UK 20 years ago [4,5]. Heat transfer rates of up to 200 W were measured under simulated UK summer conditions comparing the system favorably to conventional air conditioning and other technologies such as cooled beams. Since then, many investigations through experiments and simulations followed. A recent review [6] critically discusses experimental studies of PCM applications in buildings dividing them in free cooling passive and active methods, active and passive heating methods and hybrid applications. It describes developments in ventilation and air-conditioned systems based on PCMs as well as nano-enhanced PCMs. The extensive literature review has revealed that active LTES incorporated within the ventilation system can overcome heat exchange limitations of passive systems because of the increased heat transfer by convection and LTES is an appropriate solution to increase energy efficiency of cooling systems in buildings. A review [7] focusing on cooling LTES applications summarises experimental results of active LTES and discusses the importance of PCM selection according to cooling needs due to internal heat gains and climatic conditions. The PCM melting temperature is one of the most influencing parameters for the success of the application. Such recent reviews have also highlighted that limited analysis has been published from operational buildings with commercially installed LTES systems; such

* Corresponding author.
E-mail address: maria.kolokotroni@brunel.ac.uk (M. Kolokotroni).
[1] Permanent address: Federal Institute of Pernambuco, Av. Prof Luiz Freire, 500, Recife/PE, Brazil.

https://doi.org/10.1016/j.enbuild.2017.11.067

Nomenclature

Symbols

y_i	Measured data
$\hat{y}_i$	Simulated data
N	Sample size
$\overline{Y_s}$	Sample mean of the measured data
T_1	Cool external intake air temperature
T_2	Recirculated temperature
T_5	Temperature before thermal batteries
T_7	Temperature after thermal batteries
T_{min}	Minimum temperature
T_{max}	Maximum temperature
T_{rm}	Running mean temperature

Superscripts

N	Sample size

Abbreviations

AC	Air Conditioning
ASHRAE	American Society of Heating, Refrigerating and Air-Conditioning Engineers
CFD	Computational Fluid Dynamics
CIBSE	Chartered Institution of Building Services Engineers
COP	Coefficient of performance
CVRMSE	Coefficient of Variation of the Root-Mean-Square Error
EPP	Expanded Polypropylene
EWY	Example Weather Year
HUI	Internal Space Humidity
HVAC	Heating, Ventilation and Air Conditioning
IAQ	Indoor Air Quality
EWY	IESVE
LTES	Latent Thermal Energy Storage
MBE	Mean Bias Error
PCM	Phase Change Material
ppm	Parts per million
RH	Relative Humidity
TES	Thermal Energy Storage
LTES	Latent Thermal Energy Storage
TUI	Internal Space Temperature

results are important to accelerate inclusion in designs for new and refurbished buildings.

This paper attempts to fill part of this gap by presenting field measurements from two operational case-study rooms ventilated and cooled through a commercially available mechanical ventilation system incorporating an active LTES. Section 2 describes the ventilation unit, the two case-studies and how the system works. Section 3 presents the operational performance of the system in terms of thermal comfort, indoor air quality and energy use. Section 4 presents validated thermal and CFD models which were used to carry out parametric analysis for performance improvements. Finally, Section 5 includes the conclusions.

2. Description of the system and the case-study buildings

2.1. LTES ventilation unit

There are few technologies available on the market of LTES for free cooling and heating; one is Cool-Phase® by Monodraught Ltd. Fig. 1 shows the system investigated in this paper indicating its components consisting of a G4 filter, recirculation damper, fan, LTES and diffusers. The LTES physical size varies according to capacity (6, 8 and 10 kW) and model; 3995 mm to 5805 mm width, 966 mm depth and 400 mm height. The PCM is encapsulated in an aluminium panel available commercially [8]. Each panel holds 2 kg of PCM able to provide 88 Wh (317 kJ); each module of the LTES studied has 18 panels. Modules are put together depending on the required capacity; for the 10 kW model, the unit consists of 18 panels x 6 modules (3 modules per side) which equals to 9.5 kWh (34.2 MJ); the 8 kW model consists of 18 panels x 4 modules (2 modules per side) which equals to 6.37 kWh (22.8 MJ). An electronic system controls the damper and directs the airflow through the LTES or bypasses it through an EPP Expanded Polypropylene duct. The fan provides 260 l/s maximum during cooling mode and 300 l/s during charging mode.

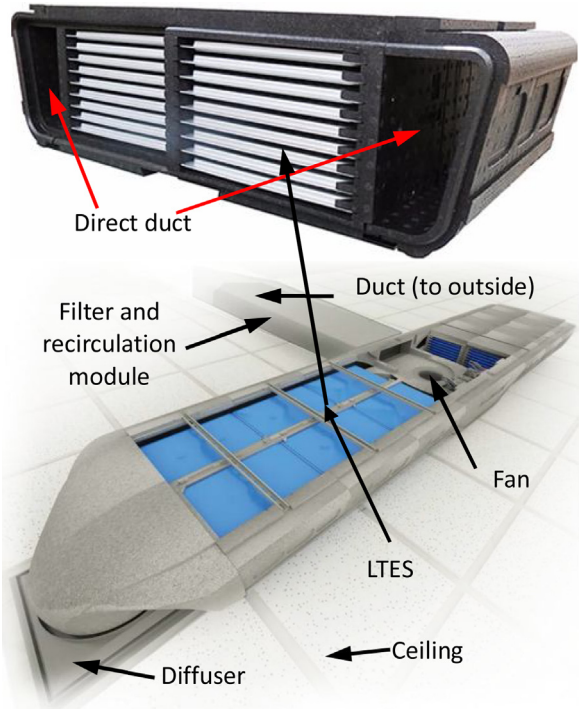

Fig. 1. Diagram of Cool-Phase® Unit [source: Monodraught Ltd].

The PCM's solidifying temperature used in LTES is limited by the temperature used to charge the material (night outside air temperature). This selection is also based on the cooling demand (lower melting point for high demand and higher melting point for lower demand) [9]. Due to this, the Salt-hydrated PCM SP 21E by Rubitherm (melting: 22–23 °C; solidifying: 21–19 °C; heat capacity: 170 kJ/kg for a temperature range of 13–28 °C) suits the studied system and its applications. Salt hydrates work by arranging and breaking the reaction salt-water (hydrate-dehydrate). They have high latent heat per unit volume, high conductivity (double of paraffin) and little volume change during melting. However, salts have a density higher than water and stay at the bottom of the container, making the freezing process more complicated [1].

The studied system is essentially a demand control ventilation and cooling system, controlled by temperature, relative humidity and CO_2 levels inside the conditioned space. A summary of the operation modes is presented in Table 1. Fig. 2 presents a schematic of the system indicating the location of the sensors used to control its operation. Temperature is controlled by either air drawn from outside or recirculated from the room; depending on the temperature and relative humidity in the conditioned space, external air is used directly or mixed with recirculated air by-passing the LTES. If cooling is needed the air is directed to the LTES. If the room exceeds metabolic CO_2 concentration limit, fresh air from outside is intro-

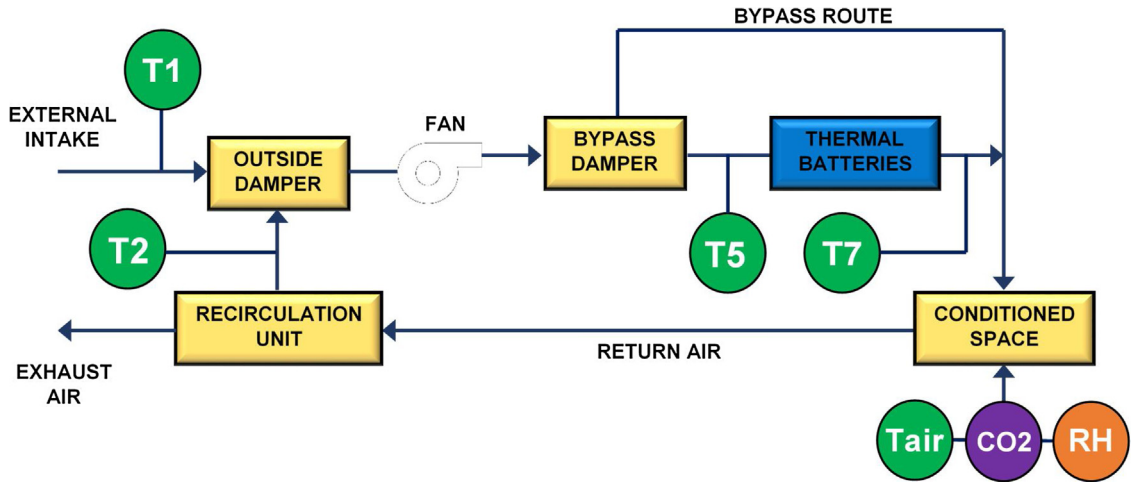

Fig. 2. Schematic of the LTES system indicating the location of the sensors analysed in this paper.

Table 1
Brief description of operation modes.

Direct outside air ventilation	Used when the outside temperature is cooler than inside, the air is supplied into the room bypassing the LTES until it reaches a set point temperature.
Outside ventilation and cooling	Used when the outside temperature is lower than inside but is not low enough to cool the space; the air crosses the LTES before entering the room.
Recirculation and cooling	When the temperature outside is higher than inside, recirculating air passes over the LTES before entering the room.
Summer Charging	During unoccupied hours, the fan supplies outside cold air to charge the LTES and release the build-up heat. When the LTES is full charged, the system turns off automatically.
Heat recovery cycle	In winter times, when the room is unoccupied or warm, the air is re-circulated through the LTES to charge and use it to reduce the heating system load.
CO_2 control	When CO_2 concentration inside is higher than a specific set point, outside air is supplied.
Humidity control	When the room relative humidity is lower or higher of a preset set point, the system will change outside air supply until the set point range is achieved.
For all modes during occupied hours, an outside minimum volume flow is provided to ensure a minimum air flow rate according to regulations	

Table 2
Default control strategy parameters.

Season	Autumn	Winter	Spring	Summer
Start Day	01-Oct	01-Dec	01-Mar	01-May
Temperature (°C)	23	24	23	22
Desired CO_2 (ppm)		900		
High CO_2 (ppm)		1200		
Charging mode		1:00 to 6:59		
Cooling mode		8:00 to 20:59		
Boost charge mode		00:00 to 00:59		

Flow Rate (l/s)	Temperature °C	CO_2 Level (ppm)	Notes	Enhanced flow rate (l/s)
300	>26		Purge	300
240	26	1800	Max under normal conditions	300
210	25	1600		260
175	24	1300		240
140	23	1000		210
100	22	900	Default min level	175
0	off	off		off

duced. The control system has default set-points but the user is able to adapt them according to needs. Table 2 presents the default set-points; air temperature varies according to the season and air-flow rate according to metabolic CO_2 and air temperature while maintaining relative humidity within a range of 30–70%.

2.2. Description of case-studies

The main case-study with the system installed is a seminar room at a university campus in West England. Similar units have been installed in many rooms (typical classrooms and offices) of the building but a seminar room was chosen because of its use (computer laboratory) with higher internal heat gains. In addition, an open plan office building is presented as a second case-study. This second case-study shows the system's performance (based only on the system's monitoring data) to indicate a range of applications.

The climate in both locations (UK, Bristol and Cambridge) is temperate maritime with 2684/2024 Heating Degree Days and 196/319 Cooling Degree Days (base 15.5 °C) [10] indicating low cooling requirements due to external conditions so cooling load is mainly determined by internal heat gains.

The main case-study was renovated into a seminar room by joining three pre-existing rooms. The existence of a plenum favoured

Table 3
Space monitoring sensors description.

Parameter Measured	Logger	Range	Accuracy	Resolution
Temperature and RH	HOBO UX100-003	−20° to 70 °C15% to 95% RH	±0.21 °C from 0° to 50 °C, ±3.5% from 25% to 85% RH	0.024 °C, 0.07% RH at 25 °C
Temperature	ibutton DS1922L	−40 °C to +85 °C	±0.5 °C from −10 °C to +65 °C	0.5 °C
CO_2	Telaire 7001	0 to 2500 ppm	±50 ppm or 5% of reading	±1 ppm

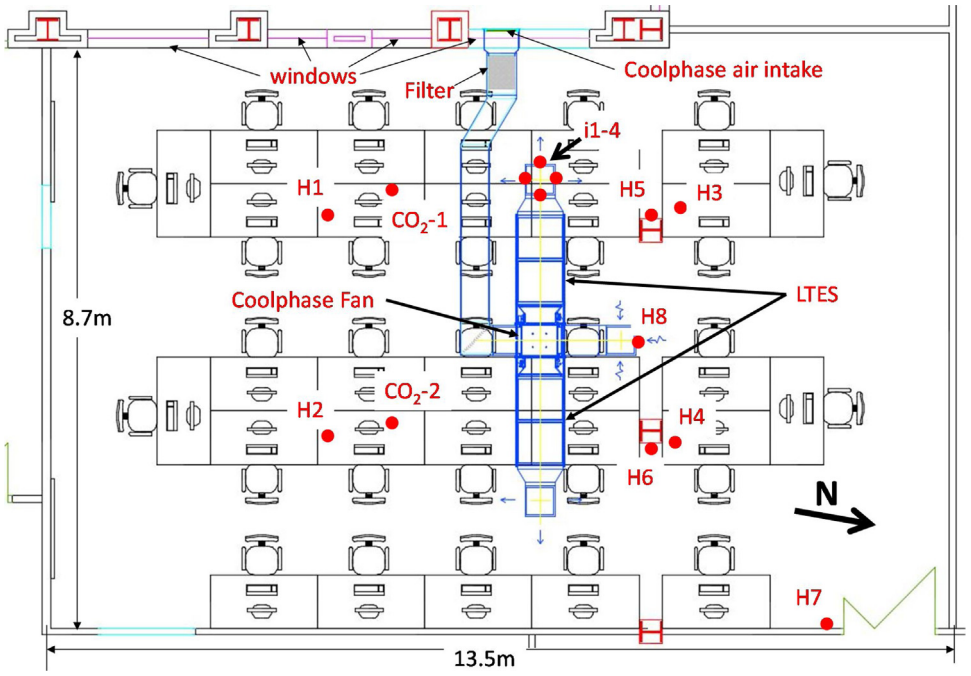

Fig. 3. Floor plan of the seminar room case-study also showing the position of the LTES unit and the position of purpose installed sensors.

the installation of the suspended ceiling system model of the system. The refurbished seminar room floor plan can be seen in Fig. 3 where the position of space monitoring sensors (for the purpose of this study) are shown. The room has a floor area of 117 m^2 and includes 29 desk top computers, peak occupancy of 29 students, and artificial lighting comprising of 24 luminaires each equipped with one 48 W lamp. The total maximum internal heat gain in the room is 60 W/m^2. The room has one external wall facing west with U-value of 0.56 W/m^2 K while 23% is glazing (overall U-value 1.82 W/m^2 K) with internal blinds. Ventilation and cooling is provided via the 10 kW LTES unit which is positioned in the middle of the room above the suspended ceiling. Heating is provided through perimeter hot water radiators and windows are openable.

The second case-study is a ground floor open plan office with a floor area of 535 m^2, housing 50 office workers with internal maximum heat gains of 45 W/m^2. Five 8 kW units (two master and 3 slaves) have been installed and can be seen on Fig. 4. The master units are directly connected to the control sensors while the slaves follow the operation of the master unit. The open plan office is one storey with external walls facing north, east and south and a pitched roof with a false ceiling. Wall U-value is 0.46 W/m^2 K, floor 0.75 W/m^2 K, roof 0.187 W/m^2 K and window 3.3 W/m^2 K with internal blinds. The area of windows is 30% of external wall area. Heating is provided through perimeter hot water radiators and windows are openable.

2.3. Description of system operation

Indicative operation of the LTES units in the two case-study spaces during summer is shown in Figs. 5 and 6 . The control system is very similar apart from differences in the times of 'day mode' due to the different use of space. A description of the operation modes is presented below:

Operation Mode 2: Night Purge-Midnight to 01:00–the fan runs at the highest speed setting for 1 h with the aim of flushing the room of stale air. Fig. 5 shows that all temperatures within this period decrease including the Internal Space Temperature, TUI. It should also noticed that T1 (external intake duct) is the temperature of the sensor placed at the face of the intake duct. This sensor can be influenced by infiltration from the room if the plenum is not well sealed. This is what happened in this case and highlights the importance of sensor position for optimum operation of the system. In the open plan office (Fig. 6) the external intake duct sensor is better positioned.

Operation mode 3: Summer Night Charge- 01:00 to 07:00–During this period, the inlet and outlet temperatures of the LTES (T5 and T7, respectively) can be seen to decrease indicating that the LTES is being 'charged' as the external intake air is being passed through them.

Operation mode 4: System Switched Off – 07:00 to 08:00–The system is turned off for 1 h in the morning in a period before the occupancy schedule begins. A crucial observation however, is that the internal space temperature (TUI) rises during this period which effectively negates some of the work done to cool the space during the night. The internal space temperature at 7:00 was well within the thermal comfort range and there was no risk of overcooling. A similar increase of internal space temperature is observed in the open plan office (Fig. 6); in this case by more than 1 °C and it may influence the timing of peak internal temperatures later in the day.

Operation mode 1: Summer Day Mode – 08:00-21:00 (seminar room) 08:00 to 18:00 (open plan office). In the seminar room (Fig. 5) the cooling mode starts at 8:00 until 21:00. In the beginning of the day (8:00–~12:00) the LTES is by-passed as the outside air is

Table 4
CO_2 concentration in the seminar room from 8:00 to 21:00.

Month	2014		2015		>1500 ppm for more than 20 min
	Avg. CO_2	Max. CO_2	Avg. CO_2	Max. CO_2	
Jan	601	1963	563	1312	0
Feb	719	2019	671	1358	1
Mar	695	2019	645	1204	0
Apr	559	2019	549	1236	0
May	469	885	443	978	0
Jun	412	607	420	531	0
Jul	409	663	420	575	0
Aug	423	580	418	826	0
Sep	493	1199	541	1326	0
Oct	599	1229	689	1268	0
Nov	701	1317	752	1480	0
Dec	551	1463	586	1551	0
Avg.	553	–	558	–	–

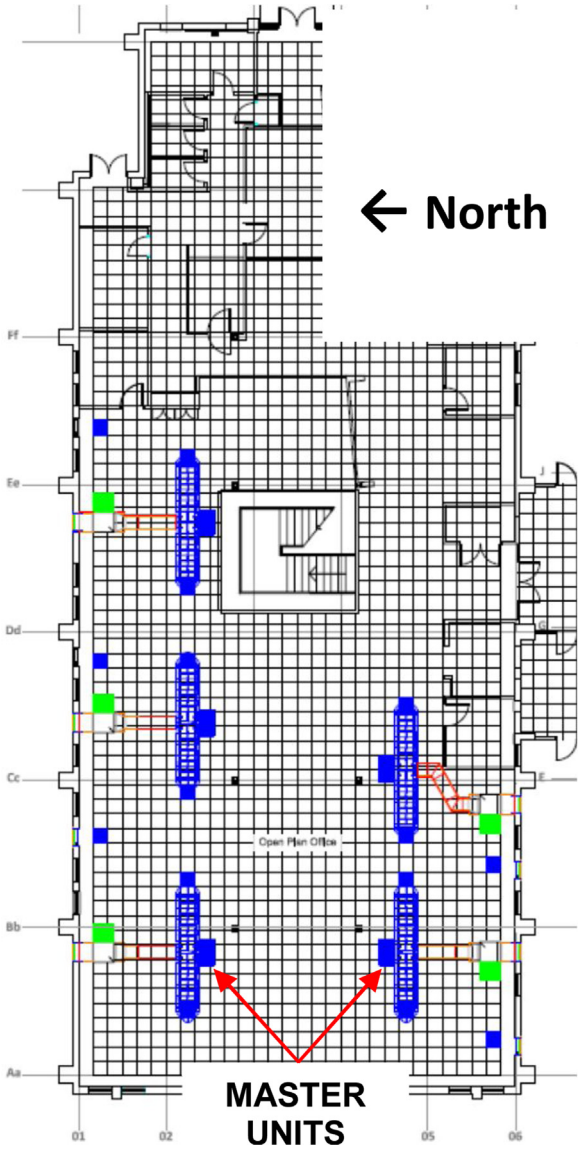

Fig. 4. Open plan office floor plan.

cooler and room temperature is below summer set-point (22 °C). At ~12:00, the external temperature measured by the external intake duct (T1) reaches the summer set-point and air is directed through the LTES maintaining air temperature in the room below external temperature. Differences between T5 and T7 from 12:00 to 21:00 confirm LTES absorbing heat and delivering cool air into the room, although complete melting must have been reached towards the end of the cooling mode.

In the open plan office (Fig. 6), the internal space temperature is above the set-point (23 °C) at 8:00, so the cooling mode is initiated. The outside air temperature is below the set-point so recirculated air is by-passing the LTES until about 10:40 when the internal temperature reaches the set-point. During this period, T5 and T7 readings are misleading as there is no air flow through the route of these sensors and so T1 is effectively the supply air temperature. At 10:40 the air is directed to the LTES and the inlet air (T7) is cooled by the melting PCM; this is shown by the sudden rise of T5 and drop of T7. The difference between T5 and T7 reaches its maximum at 17:15 with a 7.2 °C difference. Internal space temperature is maintained to below adaptive themal comfort upper limit calculated to 27.5 °C for this day (see Fig. 8).

Operation mode 4: System Switched Off – 21:00 to 00:00 (seminar room) 18:00-00:00 (open plan office) -At 21:00 or 18:00 the conditioned period in the space ends, the system switches off and all temperatures converge to the same value. The system remains switched off until midnight where the process starts again.

3. Operational performance during the year

3.1. Method

As mentioned before, data from the unit's control system were available as well as additional space monitoring inside the seminar room. These are used for the performance evaluation. Monitoring of room temperature and relative humidity was carried out within the seminar room using 8 HOBO loggers measuring for one year at 5 min interval. The position of the sensors are shown in Fig. 3. Sensors H1, H2, H3 and H4 were installed at 0.70 m from the floor, H5 and H6 at 1.80m, H7 at the same level as the system's wall mounted user control (1.5m) and H8 was placed close to exhaust grille (located on the ceiling). In addition, four ibutton loggers were placed in the inlet diffuser measuring air temperature at 5 mins interval. CO_2 measurements were taken using two Telaire sensors on two days (25–26/11/2015) to analyse CO_2 distribution and compare with system data. Sensors' specifications are presented in Table 3.

3.2. Thermal comfort analysis – summer

Adaptive thermal comfort approach is used for the evaluation during cooling season [11], as these are current guidelines for school buildings in the UK [12] and followed for non-AC office buildings [13]. The upper and lower limits of adaptive thermal com-

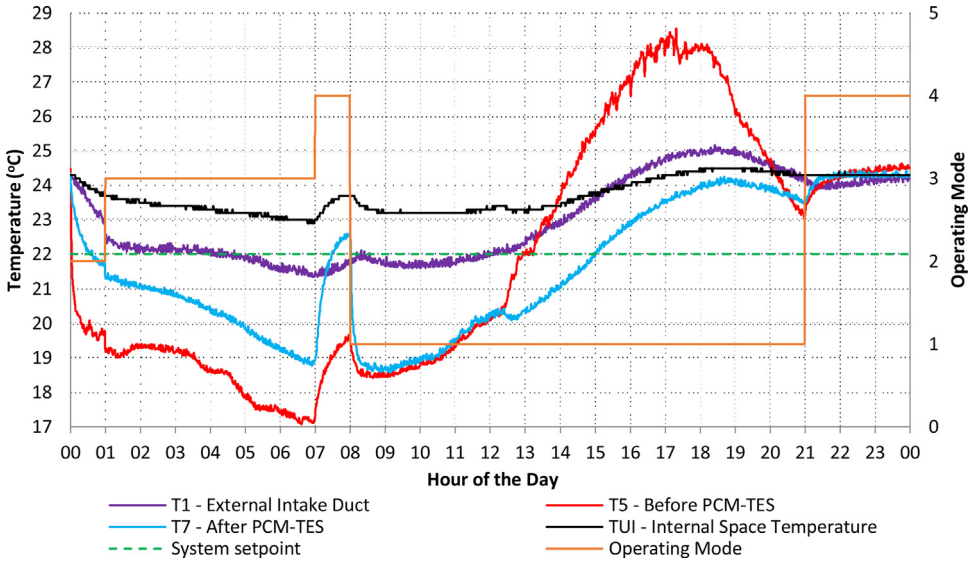

Fig. 5. Operation of LTES unit in the seminar room one day in August. (1 = cooling mode, 2 = purge mode, 3=charging mode, 4 = off).

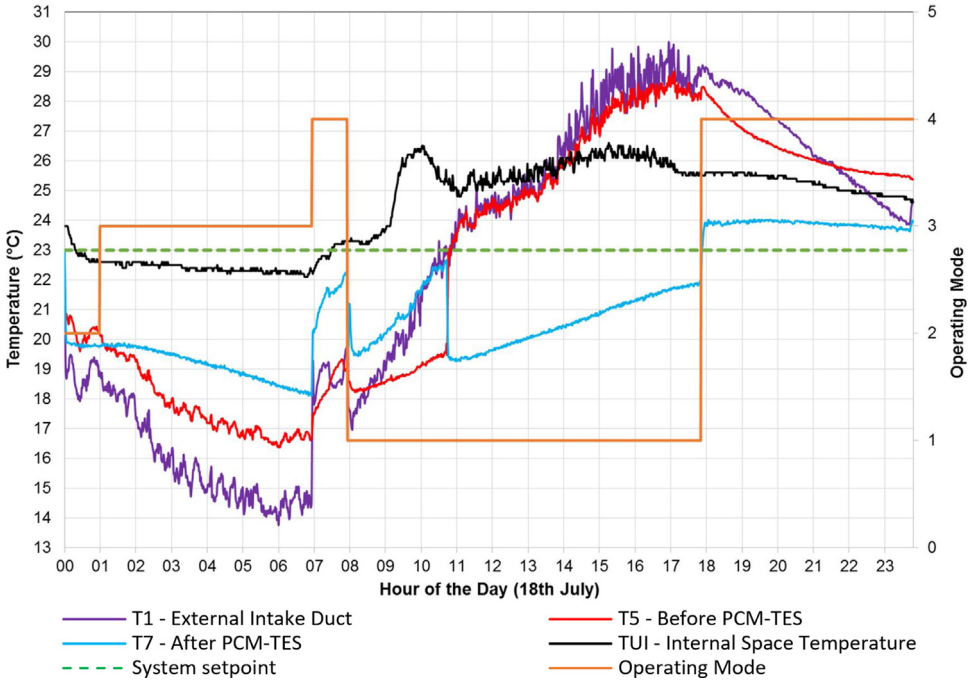

Fig. 6. Operation of LTES unit in the open plan office one day in July. (1 = cooling mode, 2 = purge mode, 3=charging mode, 4 = off).

fort are based on category II ($T_{min} = T - 3$ and $T_{max} = T + 3$) with T_{min} and T_{max} calculated by: $T = 0.33\,T_{rm} + 18.8$ where T_{rm} is the running mean external temperature. Fig. 7 shows the results during weekdays (8:00 to 21:00) for the seminar room for two summers; temperature and relative humidity is the average of all sensors at 0.7m. Relative humidity is within a good range between 30 (apart form 3 h on one day in May) and 70% (apart from one day in August). Temperature did not exceed the upper thermal limit. In general, the low solar gains because of the small area of windows and ground floor position of the room allow the system to maintain comfortable conditions during summer periods with full occupancy; for example during examination times in mid May and mid August 2016. However some overcooling occurs for some hours indicating that night purging might need more detailed control than relying on a timer; this is discussed in more detail in Section 4. Comparison of temperatures at different heights have shown no deviation from thermal comfort ranges [14].

Fig. 8 shows the system space temperature in the open plan office for one summer season. There is a gap due to lost data. The system shows very good performance with regards to the calculated thermal comfort, with very few thermal comfort limits exceedance, during one week in July (upper limit) and in May (lower limit). The exceedance in May is due to low night temperatures and during the charging at night the 18 °C night cooling limit is reached very quickly so when the system is turned off at 7:00 the increase in temperature is not enough to reach the lower limit of thermal comfort when the conditioned period begins. This behaviour of the control system is representative of the trade-off

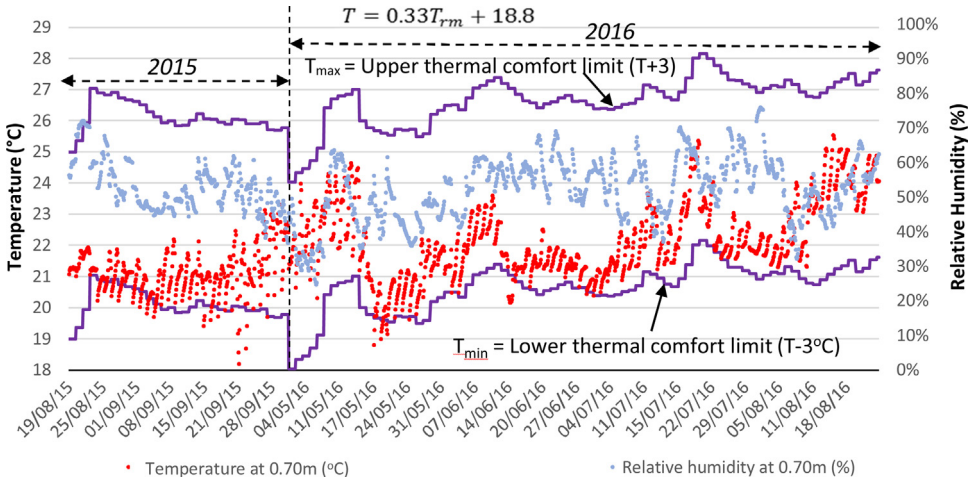

Fig. 7. Temperature and Relative Humidity at seating height in the seminar room for two summer seasons during cooling period (8:00-21:00).

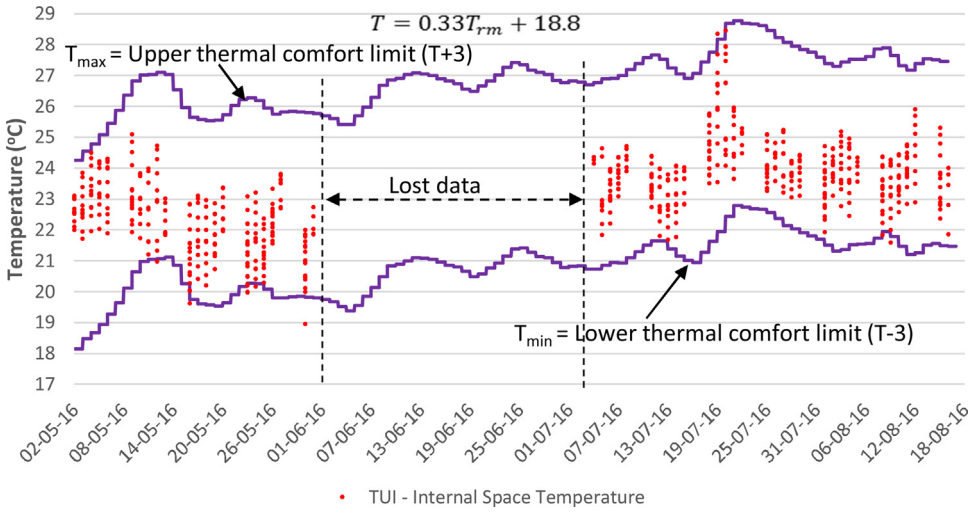

Fig. 8. Temperature in the open plan office for one summer season during cooling period (8:00-18:00).

between sufficiently charging the LTES and cooling the space during the night in preparation for optimum performance on a hot day but causing the space to be too cool for thermal comfort if the morning (and day) turns out to be unusually cold for a summer period. This is a known issue and highlighted in guidelines [13] that the lower limit of thermal comfort can sometimes be misleading for cold mornings of summer periods. As such, this characteristic of the system should not be considered as a major performance-defining downfall, but still addressed within the investigation.

3.3. Indoor air quality during winter based on metabolic CO_2

During winter, thermal comfort is provided by a separate heating system (perimeter radiators) but is controlled by the LTES central unit. Table 4 presents CO_2 levels monitored by the system during the occupied hours of 2014 and 2015 in the seminar room. Average CO_2 is below the limit of 1000 ppm for any month and 1500 ppm is exceeded by more than 20 min [15] only once (29 min in 2014) which shows a good performance in terms of IAQ. Additional CO_2 monitoring was carried out in the seminar room space. Fig. 9 shows the CO_2 distribution during two days (25–26/11/2015). It can be seen that the values were always below 1500, with the exception of one minute on 25/11/2015 where CO_2 concentration reaches 1923 ppm. Because this value cannot be observed on the second sensor, it is possible that one student has blown direct on the sensor or an unexpected error occurred.

In addition, CO_2 system data compare well with room data but a response delay was noticed (Fig. 9). This will cause the system's reaction to be delayed and could provide unnecessary air flow when the room is unoccupied. A faster response system CO_2 sensor or positioned well within occupancy space (if possible) or in the exhaust air might improve performance.

Regarding the open office, Fig. 10 shows that the limit of 900 ppm of CO_2 (maximum set-point) measured by the system data was not exceeded during the coldest months of the year (January and February) when ventilation rate is kept to a minimum. The ventilation flow rate is controlled by the system based on CO_2 monitoring within the space to ensure that the set-point is not exceeded.

3.4. LTES system energy consumption

The system includes a variable speed fan and motors to control the dampers resulting in low overall energy consumption. Electrical energy consumption in the seminar room was 91.7 kWh (0.78 kWh/m^2/annum) in 2014 and 78 kWh (0.67 kWh/m^2/annum) in

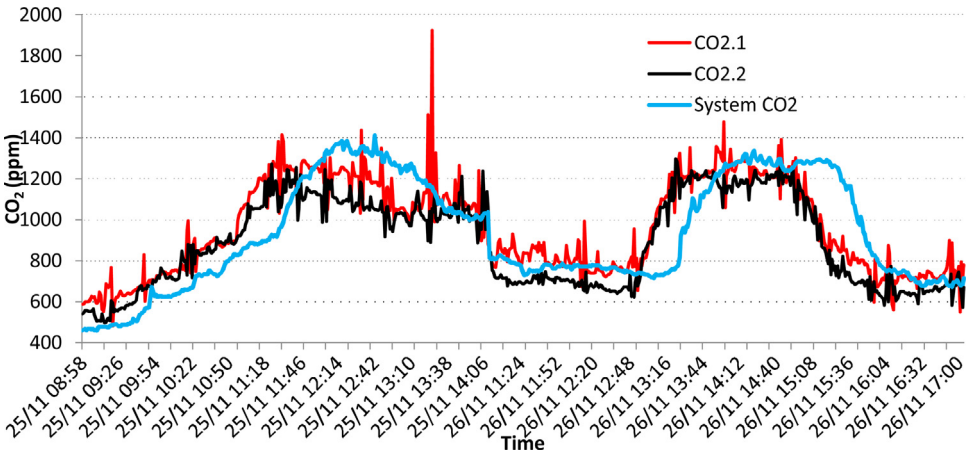

Fig. 9. CO2 measurements on two subsequent days in November in the seminar room.

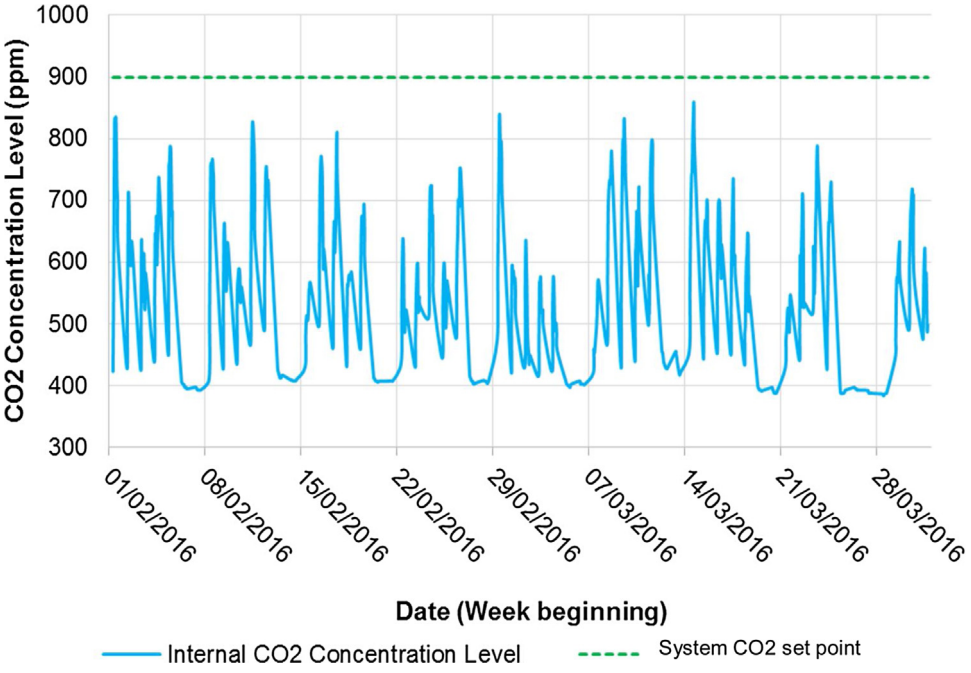

Fig. 10. CO_2 concentration in the open plan office in February and March.

2015. In monetary terms, this will cost less than £10 per year (based on 2015 cost average of £0.104 per kWh for a medium size building [16]. Simulations with IESVE (discussed in more detail in section 4) show an energy demand of 8.83 MWh to maintain the same internal conditions. Therefore, the energy used by the system is a small fraction of the energy required by an AC system (the exact saving is dependent on the AC system and its COP). Annual electricity energy use intensity for secondary schools in the UK has a median of 51 kWh/m^2 [17] including electricity used for lighting and office equipment. This increases by 5kWh/m^2 when moving from 'heating and natural ventilation' to 'heating and mechanical ventilation' buildings, indicating the typical magnitude of energy use by mechanical ventilation. CIBSE TM57 [17] presents good case-studies with cooling energy intensity of 12.5 kWh and 3.5 kWh/m^2.

In the open plan office, fan energy during the summer period (May to September) was 121 kWh (0.21 kWh/m^2). The good practice energy benchmark in the UK [18] for the cooling, fans, pumps and controls of a 'standard air conditioned office space' is 44 kWh/m^2 annually.

Therefore in both cases, energy needed to operate the system is small compared to available benchmarks.

4. Thermal and air flow modelling

The thermal simulation program IESVE [19] and ANSYS FLUENT [20] were used to carry out energy, environmental conditions and air flow simulations in the seminar room to examine the performance of the system in more detail and propose improvements. IESVE was chosen because it has a plug-in that enables the user to design the LTES system by changing parameters such as the system type, size and number of units required according to the heat gains.

4.1. Thermal modelling

The computer room model was run for one year and the accuracy was checked by comparing with measured air temperature data on an hourly and monthly basis for one year by calculating the Mean

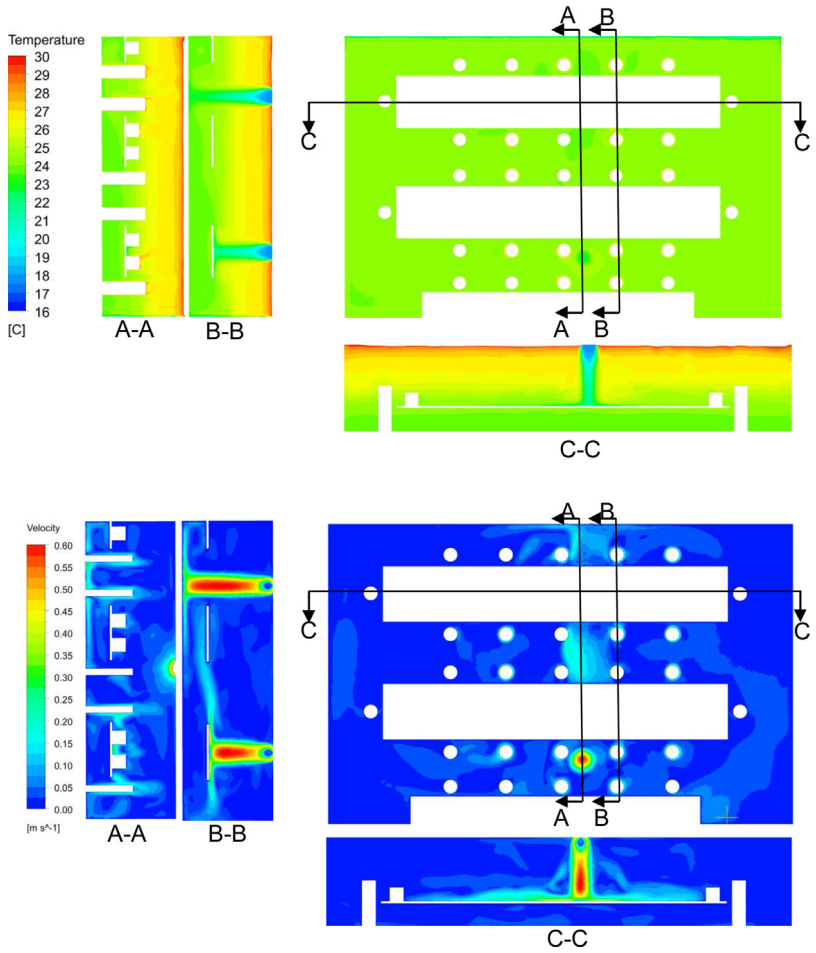

Fig. 11. CFD predictions of air temperature and air velocity at 0.70 m at 15:00pm in the seminar room.

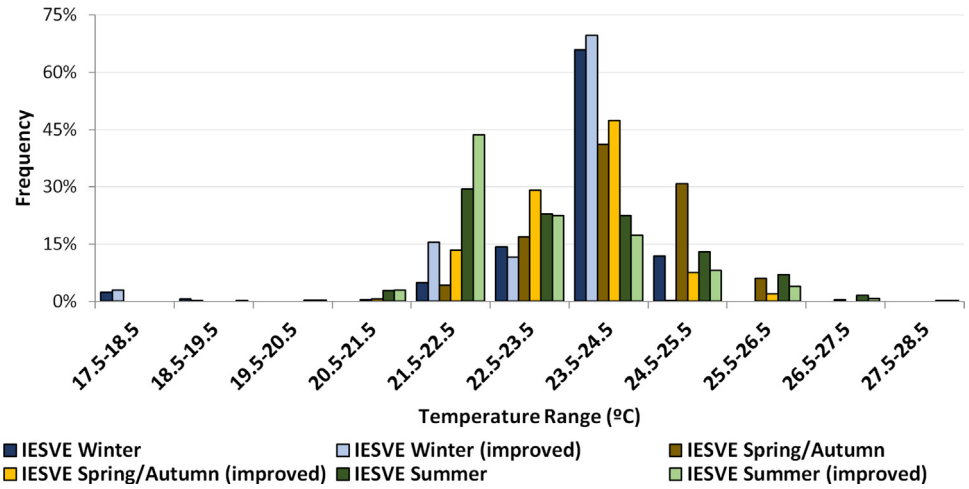

Fig. 12. Frequencies of internal air temperature with enhances air flow (see Table 2) in the seminar room.

Bias Error (MBE) and the Coefficient of variation of the Root-Mean-Square Error CV(RMSE) [21]:

$$MBE = \frac{\sum_{i=1}^{N}\left(y_i - \hat{y_1}\right)}{\sum_{i=1}^{N} y_i} \quad (1)$$

$$CV\,(RMSE) = \frac{\sqrt{\sum_{i=1}^{N}\left(y_{i-}\hat{y_1}\right)^2}/N}{\overline{Y_s}} \quad (2)$$

$$\overline{Y_s} = \frac{\sum_{i=1}^{N} y_i}{N} \quad (3)$$

y_i $and \hat{y}_i$ are measured and simulated data at instant i, respectively; $\overline{Y_s}$ is the sample mean of the measured data and N is the

Table 5
MBE and CVRSME for 2015 calibration of the seminar room.

	Jan	Feb	Mar	Apr	May	Jun	Jul	Aug	Sep	Oct	Nov	Dec
MBE	−0.59	0.68	0.09	−0.37	−0.81	−0.81	−0.29	−0.37	−0.20	−1.15	−1.21	−0.32
CVRMSE	12.93	14.84	2.10	8.49	18.27	18.28	6.76	8.38	4.67	26.33	27.15	5.81

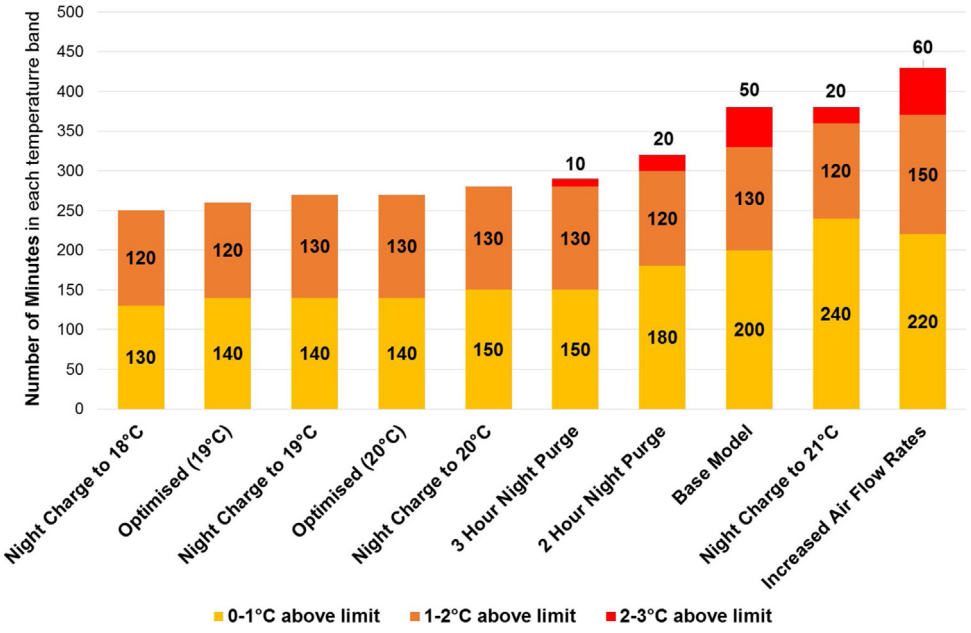

Fig. 13. Comparison of duration above thermal comfort limit for various control strategies simulated for the open plan office.

sample size (8760 for hourly based validation analysis or 12 for monthly based validation analysis.

ASHRAE Guideline 14 [21] and recent research studies [22–24] recommend to achieve a difference of less than 5% in MBE and less than 15% in CV(RMSE) between monthly prediction and measurements. When hourly data are used, a difference of 10% in MBE and 30% in CV(RMSE) is recommended as good agreement between predictions and measurements.

Weather data for the prediction period was sourced from Weather Underground [25] and introduced in simulations by updating the EWY weather file with air temperature and relative humidity data of the monitored period (2015). IESVE plug-in standard control system was improved using CO_2 data [26] to calculate the number of students and computers during operation until the simulation results for each month achieved values of MBE and CV(RSME) below 10% and 30% respectively when compared to measurements (Table 5).

The same calibration procedure was followed for the open plan office but using available data during the summer period in 2016. The MBE achieved was 2.55 and 2.65 for July and August respectively, while the CV(RMSE) was 25.52 for July and 28.42 for August.

4.2. Space temperature and air flow modelling

To analyse the system performance and propose further improvements, CFD modelling was carried out to investigate that space conditions are within thermal comfort ranges throughout the room. A 3D model of the seminar room was constructed and the day of 24/09/2015 was chosen for investigation due to the better match between room data, system data and IESVE temperature profiles. A constant air flow (100 l/s) by the system was also important to secure a uniform air distribution and a consistent CFD simulation. 100 l/s is the design air flow to operate for most of the cooling period and when occupants are accommodated (for this particular case, when students are seated). 100 l/s occur in 26.8% and 44.3% of the cooling time in 2014 and 2015 respectively. Airflows between 100 and 140 l/s in 2014 and 2015 occur in 63% and 78% of the cooling time. Heat gains from computers (11) and students (14) at 15:00 were extracted from IESVE and introduced in ANSYS FLUENT as the boundary condition. Because most of the students are seated during the class, the body (represented as a cylinder) have diameter of 0.4 m and 1.36 m of height. The body surface area of approximately 1.83 m^2 corresponds, according to DuBois [27], to a man with 1.70 height and approximately 73 kg. Thermal skin properties were introduced with a skin temperature of 33.7 °C [28], computers and lights have a temperature of 40 °C [29], tables are made of wood with zero heat flux. The room wall, ceiling and floor temperature was assumed to have the same temperature as the outer rooms and because of this the heat flux is zero. The fourth wall faced to outside building has convection as a boundary condition and the heat transfer coefficient was calculated using McAdams correlation [30] with weather data taken from Weather Underground [25].

Boussinesq approximation was used because density does not vary a high range. Radiation model was not considered on this analysis and Realizable k-e with standard wall function was chosen with second order upwind solution methods for momentum, turbulence and energy. Meshes of 580,094, 801,471, 920,117 nodes were generated and a few variation on average temperature between the last two meshes on the z plane located at 1.2 m above the floor was encountered. Due to that the mesh of 801,471 nodes was used.

Results of this simulation are presented in Fig. 11 where a plane at seated level (0.70m) shows an average of 24.21 °C, 1.62 °C higher (or 7.14%) from room data at the same height. This is a reasonable result; the indoor environmental modelling chapter of ASHRAE fundamentals [31] indicates that a difference of 20% could be considered excellent for complex flow problems. Fig. 11 also shows that at 0.70m, no thermal discomfort is expected based on the adaptive thermal comfort limits. Air velocity contours show a range of

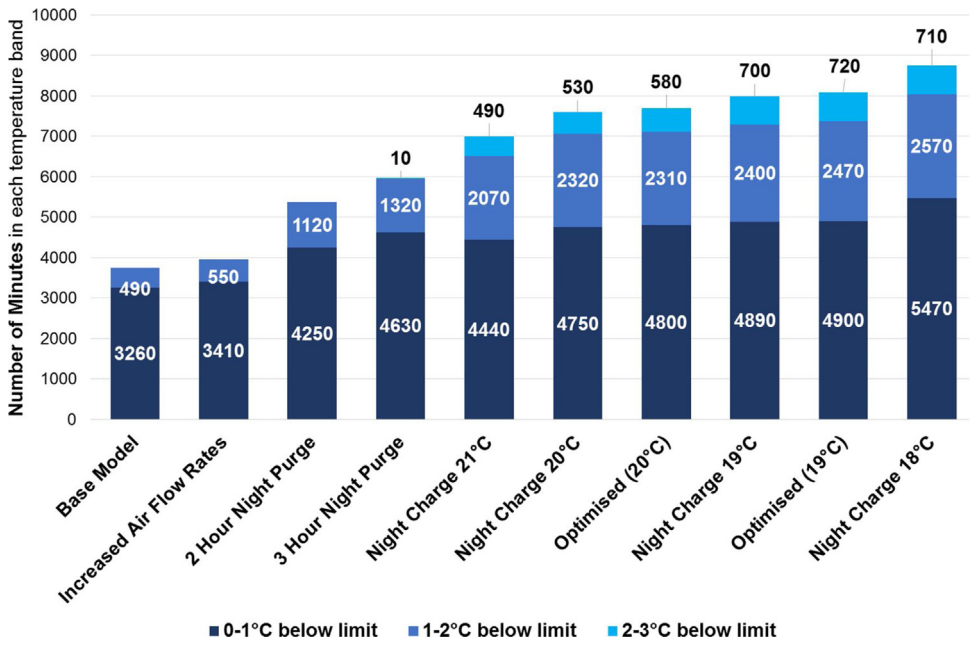

Fig. 14. Comparison of duration below thermal comfort limit for various control strategies simulated for the open plan office.

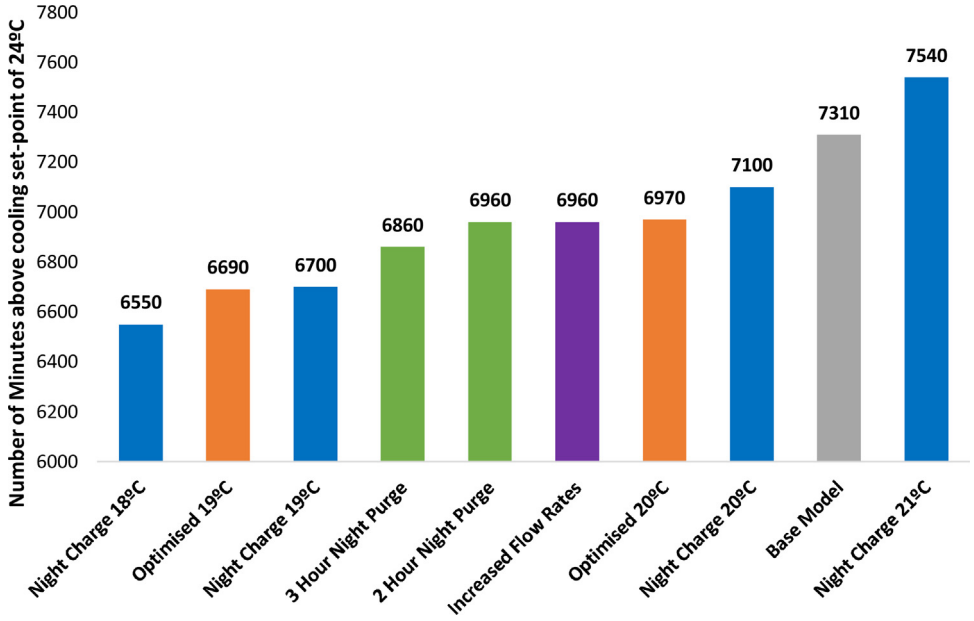

Fig. 15. Comparison of duration above system set-point for various control strategies simulated for the open plan office.

0.1–0.2 m/s within the space apart from a small area near or directly under the air inlet.

4.3. Parametric analysis for performance improvements

With the calibrated models, parameters in IESVE were adjusted and improvements on system performance can be tested with confidence.

4.3.1. Increased air flow rate

Improvements in the computer room were simulated. The question investigated is whether air flow rate increases will improve IAQ and reduce CO_2 levels and whether this might affect thermal comfort and energy use negatively. This was investigated by increasing the airflow at each temperature set-point (see Table 2). The results presented in Fig. 12 indicate increased percentage of air temperature inside the summer, autumn/spring and winter set-points. For the summer period, 43.6% of hourly temperatures are inside the set-point range (22 °C ± 0.5 °C) an increase of 14.2%. During the autumn there was also an increase of 12.3% of hourly temperatures inside the set point temperature (23 °C ± 0.5 °C) while temperatures above 24.5 °C had a significant reduction of 27.7%. During winter, temperatures were at set point of 24 °C (±0.5 °C) for 69.6% of the time, an increase of 3.7%. For the whole year, the base-case model present temperatures inside the season set-point range for 37.4% and the model with enhanced air flow rates 47.4%. This increase in air flow rate of approximately 10% will consume additionally 44 kWh per year (or 51.4%) which is a small penalty despite the high increase in percentage value.

4.3.2. Timing and set points of night purge and night charge modes

Improvements during the summer period in the open plan office were investigated. Summer is the target period for cooling in the offices as IAQ assessment based on metabolic CO_2 is less important than in the seminar room because of the much lower occupancy density. A parametric analysis was carried out changing timing and set points of the operational modes described in section 2, as follows:

- Night Purge-extended to 2 and 3 h.
- Summer Night Charge-extended; no system shut-off period and varying set points of internal temperature (18 °C, 19 °C, 20 °C, and 21 °C).

The main aim was to reduce peak internal temperatures and time spent above the upper limit of thermal comfort. Fig. 13 presents the results showing the reduction in temperature frequencies above the upper thermal comfort limit over a 3 day period; July 20th-22nd. With the exception of the 21 °C target temperature, the extended night charge modes provide the best improvements in comparison to the base model, with the largest reduction of 130 min (34%) by the extended night charge with 18 °C internal target temperature. However the night charges to 19 °C and 20 °C, as well as the 2 optimised simulations, have very similar reductions. As the modified night charge and purge modes were effective and achieving a lower PCM temperature, it was considered that involving the increased air flow rates within the combined simulations might mitigate the rate at which the PCM rose in temperature, which led to an increase in peak internal temperatures. This was trialled but the same impact of the increased air flow rates was realised due to the small temperature differential.

To increase the cooling capacity any further, other elements of the system (such as the shape of the heat exchange surfaces or the PCM itself) must first be developed to increase the heat transfer rates of the thermal batteries, and thus improve thermal comfort. This is an area of current investigation by the authors. However, as the simulations analysed in the parametric analysis do achieve a positive influence on the time spent below the upper thermal comfort limit, it is predicted that these improvements to performance will be amplified with any increase in system cooling capacity.

Despite the benefits that are recognised throughout the analysis, there are consistent disadvantages in the frequency and magnitude of breaches of the lower thermal comfort limit (Fig. 14). The general trend shows that the results with most notable reductions in time spent above the upper limit, also tend to acquire the most breaches of the lower limit. These are found to occur within the first 2 h of the conditioned period due to the modified night modes cooling the space to a lower temperature. Some of these occurrences are also found to be unavoidable, even by the Base model, when the system does not even activate during the night period and the limit is still breached. As mentioned before this is a point raised in the literature [13] about the lower limit of adaptive thermal comfort calculations which can be overcome with behavioural adjustments.

4.3.3. Increased flow rates in the open plan office

A summary of the performances in relation to cooling set-point and increased flow rate is presented in Fig. 15. The results show a similar trend to those concerning the upper thermal comfort limit (Fig. 13) with the exception of the 3 h night purge and increased air flow rates simulations providing better performance compared to the other strategies than they did for peak temperatures. Increasing the air flow rates means that cool air can be provided at a faster rate and control the internal temperatures more effectively, however the downside to this was that during peak temperatures, the thermal batteries losing their cooling capacity too early within the occupied period to cope with peak temperatures. In nearly all the analysis conducted, the extended night charge to 21 °C was shown to perform worse than the Base model as it was shown that it did not provide sufficient cooling of the space or charging of the thermal batteries to control the internal conditions as effectively.

In terms of energy consumption for the fan, the optimised strategy to 19 °C with increased air flow rate results to an increase in energy consumption of 168 kWh for the whole summer period (May–September 2016). This increase equates to 0.31 kWh/m^2 fan energy consumption compared to 0.21 kWh/m^2 of the base case, an increase of approximately 48%.

5. Conclusions

This paper presented an active ventilation cooling system that can be suitable for newly built and retrofit applications. The system is a mechanical ventilation system which uses PCM thermal storage in the ventilation path and utilise night cool air for solidifying the PCM which in turn cools recirculated or external air during its melting phase. The two case-studies presented are both retrofit applications; a seminar computer room (with internal heat gains of 60 W/m^2) and an open plan office (with internal heat gains of 45 W/m^2). The system was installed in the existing plenum of the space with access to outside. Detailed monitoring of the spaces and thermal/CFD analysis indicated that the system can provide acceptable thermal comfort throughout at seating occupant level (0.7 m from the floor) in the moderate weather summer conditions of south and west England using adaptive thermal comfort limits.

A parametric analysis was carried out to investigate possible improved performance by an optimised control strategy. It was found through simulations that increasing air flow will keep internal temperatures more frequently within the set-point range without compromising thermal comfort and indoor air quality with a small electricity increase penalty. Considering the increase of night purge duration and charging in relation to room air temperatures, the maximum improvement to thermal comfort was obtained by increasing air flow rates with an extended night purge of 3 h and extended night charge mode with a night time internal space target temperature of 20 °C that runs through until the occupied period. This strategy achieved an improvement which is 3% less than the biggest reduction in the time spent over the upper thermal comfort limit achieved by the extended night charge with a target temperature of 18 °C. The control proposed also achieves smallest time spent below the lower thermal comfort limit, with 21% less time spent below the limit compared to the strategy of night charge to 18 °C.

The analysis indicated that changes in the control strategy improve the performance of the system. However, this is limited by the cooling capacity of the PCM. One solution is to increase the PCM material but this will result to larger space requirements. Another solution is to increase the heat transfer rate of the existing configuration; further research will investigate this numerically and experimentally by examining the geometry of encapsulation and stacking density in relation to pressure drop and cost of production.

Acknowledgements

The first author would like to thank Science Without Borders program of CNPq – Brazil, for doctoral funding (PDE: 200815/2014-8). Thanks are also due to Mitch Neksojevic who facilitated the installation of monitoring equipment in the seminar room.

References

[1] A. Sharma, V.V. Tyagi, C.R. Chen, D. Buddhi, Review on thermal energy storage with phase change materials and applications, Renew. Sustain. Energy Rev. 13 (2009) 318–345, http://dx.doi.org/10.1016/j.rser.2007.10.005.

[2] M. Aneke, M. Wang, Energy storage technologies and real life applications –a state of the art review, Appl. Energy 179 (2016) 350–377, http://dx.doi.org/10.1016/j.apenergy.2016.06.097.

[3] M. Labat, J. Virgone, D. David, F. Kuznik, Experimental assessment of a PCM to air heat exchanger storage system for building ventilation application, Appl. Therm. Eng. 66 (2014) 375–382, http://dx.doi.org/10.1016/j.applthermaleng.2014.02.025.

[4] J.R. Turnpenny, D.W. Etheridge, D.A. Reay, Novel ventilation cooling system for reducing air conditioning in buildings, Appl. Therm. Eng. 20 (2000) 1019–1037, http://dx.doi.org/10.1016/S1359-4311(99)00068-X.

[5] J.R. Turnpenny, D.W. Etheridge, D.A. Reay, Novel ventilation system for reducing air conditioning in buildings. Part II: testing of prototype, Appl. Therm. Eng. 21 (2001) 1203–1217, http://dx.doi.org/10.1016/S1359-4311(01)00003-5.

[6] A. Kasaeian, L. Bahrami, F. Pourfayaz, E. Khodabandeh, W.-M. Yan, Experimental studies on the applications of PCMs and nano-PCMs in buildings: a critical review, Energy Build. 154 (2017) 96–112, https://doi.org/10.1016/j.enbuild.2017.08.037.

[7] F. Souayfane, F. Fardoun, P.H. Biwole, Phase change materials (PCM) for cooling applications in buildings: a review, Energy Build. 129 (2016) 396–431, http://dx.doi.org/10.1016/j.enbuild.2016.04.006.

[8] Rubitherm GmbH. Rubitherm n.d. https://www.rubitherm.eu/en/index.php/productcategory/makroverkaspelung-csm (Accessed November 25, 2017).

[9] A. Lazaro, P. Dolado, J.M. Marín, B. Zalba, PCM–air heat exchangers for free-cooling applications in buildings: experimental results of two real-scale prototypes, Energy Convers. Manag. 50 (2009) 439–443, http://dx.doi.org/10.1016/j.enconman.2008.11.002.

[10] Vesma n.d. http://vesma.com/(Accessed November 25, 2017).

[11] Ds/En. DS/EN 15251, Indoor Environmental Input Parameters for Design and Assessment of Energy Performance of Buildings Addressing Indoor Air Quality, Thermal Environment, Lighting and Acoustics, 2007, pp. 3.

[12] Education Funding Agency, Baseline Designs for Schools, Environmental Services Strategy and Ventilation Strategy, 2014, https://www.gov.uk/government/publications/psbp-baseline-designs (Accessed November 28, 2017).

[13] F. Nicol, B. Spires, The Limits of Thermal Comfort: Avoiding Overheating in European Buildings TM52: 2013, 2013.

[14] T. Santos, N. Hopper, M. Kolokotroni, Performance in practice of a ventilation system with thermal storage in a computer seminar room, in: CLIMA 2016, 12th CLIMA REHVA World Congr., Aalborg, Denmark, 2016.

[15] Education Funding Agency, Priority School Building Programme: Facilities Output Specification, 2013.

[16] Department of Energy & Climate Change, Gas and Electricity Prices in the Non-domestic Sector, 2013, https://www.gov.uk/government/statistical-data-sets/gas-and-electricity-prices-in-the-non-domestic-sector (Accessed June 21, 2015).

[17] A. Bissell, E. Burman, R. Daniels, D.M. Entwisle, P. Eslinger, D.B. Jones, et al., Integrated School Design TM 57, CIBSE, London, 2015.

[18] CIBSE, Guide F. Energy Efficiency in Buildings, 2012.

[19] IESVE, Integrated Environmental Solutions, IESVE, 2016, https://www.iesve.com/(Accessed November 28, 2017).

[20] ANSYS, ANSYS FLUENT Theory Guide, 2016.

[21] ANSI/ASHRAE, Measurement of Energy and Demand Savings, ASHRAE Guidel., 2002, pp. 170 (14–2002).

[22] M. Royapoor, T. Roskilly, Building model calibration using energy and environmental data, Energy Build. 94 (2015) 109–120, http://dx.doi.org/10.1016/j.enbuild.2015.02.050.

[23] G. Mustafaraj, D. Marini, A. Costa, M. Keane, Model calibration for building energy efficiency simulation, Appl. Energy 130 (2014) 72–85, http://dx.doi.org/10.1016/j.apenergy.2014.05.019.

[24] D. Coakley, P. Raftery, M. Keane, A review of methods to match building energy simulation models to measured data, Renew. Sustain. Energy Rev. 37 (2014) 123–141, http://dx.doi.org/10.1016/j.rser.2014.05.007.

[25] Weather Underground www.wunderground.com (Accessed November 25, 2017).

[26] T. Labeodan, W. Zeiler, G. Boxem, Y. Zhao, Occupancy measurement in commercial office buildings for demand-driven control applications – a survey and detection system evaluation, Energy Build. 93 (2015) 303–314, http://dx.doi.org/10.1016/j.enbuild.2015.02.028.

[27] J.F. Nicol, M.A. Humphreys, Adaptive thermal comfort and sustainable thermal standards for buildings, Energy Build. 34 (2002) 563–572, http://dx.doi.org/10.1016/S0378-7788(02)00006-3.

[28] A. Zolfaghari, M. Maerefat, A new simplified thermoregulatory bioheat model for evaluating thermal response of the human body to transient environments, Build. Environ. 45 (2010) 2068–2076, http://dx.doi.org/10.1016/j.buildenv.2010.03.002.

[29] L. Lei, S. Wang, T. Zhang, Inverse determination of wall boundary convective heat fluxes in indoor environments based on CFD, Energy Build. 73 (2014) 130–136, http://dx.doi.org/10.1016/j.enbuild.2013.12.056.

[30] W.H. McAdams, Heat Transmission (McGraw-Hill Series in Chemical Engineering), McGraw-Hill, 1954.

[31] ASHRAE, ASHRAE Fundamentals, ASHRAE, Atlanta, GA, 2013, vol. 1. SI edition.